Journal of Controlled Release 169 (2013) 239–245

Contents lists available at SciVerse ScienceDirect

Journal of Controlled Release

journal homepage: www.elsevier.com/locate/jconrel

NANOMEDICINE

Targeted biodegradable dendritic MRI contrast agent for enhanced tumor imaging

Mingzhou Ye [a], Yue Qian [b], Jianbin Tang [a,*], Hongjie Hu [b], Meihua Sui [a], Youqing Shen [a,**]

[a] Key Laboratory of Biomass Chemical Engineering of Ministry of Education and Center for Bionanoengineering, Department of Chemical and Biological Engineering, Zhejiang University, Hangzhou, Zhejiang 310027, China
[b] Department of Radiology, Sir Run Run Shaw Hospital (SRRSH) of School of Medicine, Zhejiang University, Hangzhou, Zhejiang 310027, China

ARTICLE INFO

Article history:
Received 16 October 2012
Accepted 31 January 2013
Available online 9 February 2013

Keywords:
Dendrimer
Biodegradability
MRI
Contrast agent
Tumor imaging

ABSTRACT

Highly sensitive and safe contrast agents (CAs) are essential for magnetic resonance imaging (MRI) to achieve accurate tumor detection and imaging. Dendrimer-based macromolecular MRI contrast agents are advantageous owing to their tumor-targeting ability, enhanced imaging contrast and enlarged imaging window. However, most of them have drawbacks of non-degradability and thereby long-term retention in body and toxicity. Herein, a tumor-targeting biodegradable dendritic CA (DCA) (FA-PEG-G2-DTPA-Gd) was prepared from a polyester dendrimer conjugated with gadolinium (Gd) chelates and PEG chains with distal folic acid. The DCA had a high longitudinal relaxivity up to 17.1 mM^{-1} s^{-1}, 4 times higher than the clinically used CA Magnevist. The MRI contrasted by FA-PEG-G2-DTPA-Gd outlined the inoculated tumor more clearly, and had much higher contrast enhancement for a much longer time than Magnevist. More importantly, the biodegradable FA-PEG-G2-DTPA-Gd gave much less Gd retentions in all the organs or tissues than non-degradable DCAs. Thus, the high efficiency in MRI contrast enhancement and low Gd retention merit it a promising CA for contrast enhanced tumor MRI.

1. Introduction

Cancer diagnosed in early stage can be cured by surgery, chemotherapy and other therapies, but late stages are highly lethal [1,2]. Therefore, early and accurate diagnosis of tumor is the key to decrease tumor mortality [3]. Magnetic resonance imaging (MRI) is an effective noninvasive approach to detect solid tumors [4,5], owing to its superior tissue resolution, abundant diagnostic information and absence of radiation damages.

MRI often requires contrast agents (CAs) to improve its sensitivity [6,7]. Currently used MRI CAs are mainly small molecular paramagnetic gadolinium (Gd) chelates such as diethylenetriaminepentaacetic acid-Gd (DTPA-Gd, Magnevist) [8] and Gd-diethylenetriaminepentaacetic acid bismethylamide (Gd-DTPA-BMA, Omniscan) [9]. These CAs suffer drawbacks including low longitudinal relaxivity (R_1), non-specificity, and short blood circulation times [10]. Macromolecular Gd chelates, especially dendrimer-based Gd chelates, have higher relaxivities and longer blood circulation times than the small molecular CAs, and are capable of preferential accumulation in tumors via the enhanced permeability and retention (EPR) effect [11], making them promising for tumor MRI [12,13]. Among them, Gd-conjugated polypropyleneimine (PPI) and polyamidoamine (PAMAM) have been widely investigated for tumor imaging to differentiate benign and malignant tumors [14], tumor angiogenesis [15,16], and early tumor responses to therapy [17,18]. Targeting groups were also introduced onto these dendritic contrast agents (DCA) to confer them active tumor-targeting ability to further increase the contrast-enhanced MRI [19]. For example, PAMAM-DTPA-Gd^{3+} conjugated with folic acid as targeting group was taken up preferentially by tumor cells, leading to an increase of over 100% in the R_1 of tumor cells and a 33% increase in the contrast enhancement of ovarian tumors compared with the non-targeting DCA [20,21].

However, PPI and PAMAM are not biodegradable, and thus their DCAs made from high generations cannot be effectively excreted from the body. For instance, 80% of the injected PAMAM-G6 based DCA was retained in the body after 2 days, and even after 10 days more than 10% of the dose was still in the body [22,23]. The remained CAs in the body might be internalized by healthy cells and metabolized into toxic Gd^{3+} ions, causing problems [24,25]. For instance, many recent reports linked nephrogenic systemic fibrosis (NSF) to the use of the acyclic gadolinium chelates, e.g. DTPA-Gd, [26]. To solve the problems, biodegradable macromolecular MRI CAs were developed in the past years. Lu et al. designed a series of polydisulfide MRI agents, which could be degraded by intracorporal thiol through the thiol-disulfide exchange reaction [27–29]. These degradable CAs had the merits of macromolecular CAs including relative long blood circulation time and tumor targeting by EPR effect. On the other hand, these MRI CAs could be readily degraded in physiological environment, and excreted out of the body after imaging, avoiding the toxicity problem due to Gd accumulation. However, the linear biodegradable macromolecular CAs had a wide distribution in molecular weight (Mw), leading to heterogenous pharmacokinetics of CAs.

Recently, we developed a facile synthesis of biodegradable polyester dendrimers from sequential click coupling of asymmetrical monomers

* Corresponding author. Tel./fax: +86 571 8795 3925.
** Corresponding author. Tel./fax: +86 571 8795 3993.
E-mail addresses: jianbin@zju.edu.cn (J. Tang), shenyq@zju.edu.cn (Y. Shen).

0168-3659/$ – see front matter © 2013 Elsevier B.V. All rights reserved.
http://dx.doi.org/10.1016/j.jconrel.2013.01.034

[30], and the synthesis was further simplified by using β-cyclodextrin core, from which polyester dendrimers with high molecular weights could be easily synthesized in fewer steps without intensive purifications [31]. Unlike the linear polymers, the dendrimers had identical spherical structure and monodispersed molecular weights. The MRI CAs prepared from these polyester dendrimers had high R_1 values and prominent blood pool contrast enhancement [31]. Herein, PEG and folic acid, a ligand targeting overexpressed folate receptor on most cancer cells, were introduced onto the polyester DCAs to achieve a tumor-targeting biodegradable DCA (Fig. 1). We expected that this DCA would significantly improve the sensitivity of tumor imaging by MRI without the long-term Gd-retention problem.

2. Materials and methods

2.1. Materials and measurements

Ethylenediamine and all the organic solvents were purchased from Sinopharm Chemical Reagent Co., Ltd. (Shanghai, China). Dimethyl sulfoxide (DMSO) was purified by distillation under vacuum over calcium hydride. α-Hydroxy-ω-allyl-poly(ethylene glycol) (allyl-PEG-OH, Mn = 2000) was purchased from Hai'an Petrochemical Plant (Jiangsu, China). Gadolinium chloride hexahydrate ($GdCl_3 \cdot 6H_20$) was bought from Alfa Aesar (Ward Hill, MA, USA). The cellulose ester dialysis membrane (molecular weight cut off, MWCO = 10000) was purchased from Spectrum Laboratories Inc., (Rancho Dominguez, CA). Amicon Ultra-15 centrifugal filter devices (MWCO = 10000) was purchased from Millipore (Cork, Ireland).

^{1}H NMR spectra were recorded on a Bruker Advance DRX-400 NMR spectrometer at room temperature. The sizes (hydrodynamic diameters) of the DCAs were measured using a dynamic light scattering instrument (Zetasizer Nano ZS, Malvern Instruments, UK). The concentrations of Gd^{3+} solutions from tissues were measured by inductively coupled plasma mass spectrometry (ICP-MS, XSeries II, Thermo Scientific, MA, USA).

2.2. Synthesis of FA-PEG-SH

2.2.1. Allyl-PEG-NH_2

The allyl-PEG-NH_2 was first synthesized using the method reported in literature [32,33] (Fig. 1). Allyl-PEG-OH (10.0 g, 5.00 mmol) and triethylamine (TEA, 3.97 mL, 20.0 mmol) were dissolved in 50 mL dichloromethane (DCM) at 0 °C. Tosylchloride (3.81 g, 20.0 mmol) was dissolved in 20 mL DCM, and then added dropwise into the mixture. After reacted at room temperature for 6 h, the solution was washed with water, concentrated by rotary evaporation, and poured into diethyl ether to precipitate out the solid product. The solid product allyl-PEG-OTs was dissolved in DCM and reprecipitated in diethyl ether for 3 times. The residue was dried under vacuum, giving product allyl-PEG-OTs in a yield of 9.80 g (91% yield). The purified allyl-PEG-OTs (8.72 g, 4.09 mmol) was dissolved in ethylenediamine (30 mL, 0.449 mol) and refluxed under nitrogen at 85 °C for 4 h. The resultant mixture was dissolved in DCM, washed with water, and then poured into hexane to precipitate out the solid product. The product was purified by redissolving in DCM and reprecipitating in hexane for 3 times. The solid product allyl-PEG-NH_2 was obtained after drying under vacuum with a yield of 7.98 g (95%). ^{1}H NMR in $CDCl_3$, δ_{ppm}: 5.88 (m, 1H, CH_2═CH–CH_2–), 5.24 (d, 1H, HCH═CH–CH_2–), 5.15 (d, 1H, HCH═CH–CH_2–), 4.00 (d, 2H, CH_2–CH–CH_2–), 3.62 (s, 186H, –CH_2–O–CH_2–), 2.77 (q, 4H, –CH_2–NH–CH_2–), and 2.67 (t, 2H, NH_2–CH_2–).

2.2.2. NH_2-PEG-SH

Allyl-PEG-NH_2 (7.94 g, 3.89 mmol), azodiisobutyronitrile (AIBN, 1.09 g, 6.64 mmol) and ethylenedithiol (3.27 mL, 38.9 mmol) were dissolved in 80 mL ethanol under nitrogen protection. The solution was sealed and reacted at 70 °C for 12 h. The solution was poured into diethyl ether to precipitate out the solid product. The product was isolated and purified by redissolving in ethanol and reprecipitating in diethyl ether for 5 times. The solid was dried under vacuum, giving NH_2-PEG-SH product with a yield of 90% (7.48 g). ^{1}H NMR in $CDCl_3$, δ_{ppm}: 3.62 (s, 186H, –CH_2–O–CH_2–), 3.12 (s, 2H, –CH_2–CH_2–CH_2–O–), 2.96 (s, 2H, SH–CH_2–), 2.84 (m, 4H, –CH_2–NH–CH_2–), 2.72 (t, 2H, NH_2–CH_2–), 2.62 (t, 2H, SH–CH_2–CH_2–), 2.40 (t, 2H, –S–CH_2–CH_2–), and 1.85 (t, 2H, –S–CH_2–CH_2–).

2.2.3. OH-PEG-SH

Similarly, OH-PEG-SH was synthesized following the same procedure from allyl-PEG-OH and ethylenedithiol with a yield of 85%. ^{1}H NMR in $CDCl_3$, δ_{ppm}: 3.65 (m, 188H, –CH_2–O–CH_2–), 2.87 (m, 4H, SH–CH_2–CH_2–), 2.64 (t, 2H, –S–CH_2–CH_2–), and 1.87 (t, 2H, –S–CH_2–CH_2–).

2.2.4. FA-PEG-SH

The activation of folic acid (FA) followed a reported method [34] with minor modification. FA (1.00 g, 2.27 mmol), *N*-hydroxysuccinimide (NHS, 0.287 g, 2.49 mmol), *N*′-(3-dimethylaminopropyl)-*N*-ethylcarbodiimide hydrochloride (EDC·HCl, 0.498 g, 2.61 mmol) and TEA (0.379 mL, 2.72 mmol) were dissolved in 10 mL dried DMSO under N_2 protection, and reacted at room temperature in dark for 12 h. NH_2-PEG-SH (4.84 g, 2.27 mmol) dissolved in 10 mL DMSO was then added into the reaction solution, and stirred for another 12 h under the same condition. The reacted mixture was poured into 150 mL DCM. The solution was washed with water, concentrated by rotary evaporation, and then poured into diethyl ether. The precipitate was collected by filtration and dried under vacuum, giving the product FA-PEG-SH (5.11 g, 88% yield). ^{1}H NMR in $CDCl_3$, δ_{ppm}: 8.62 (s, 0.7H), 8.06 (s, 0.7H), 7.61 (d, 1.4H), 7.00 (t, 0.7H), 6.61 (d, 1.4H), 4.45 (d, 1.4H), 4.27 (q, 0.7H) 4.00 (q, 1.4H), 3.48 (s, 184H), 3.03 (t, 2H), 2.90 (m, 6H), 2.76 (t, 2H), 2.55 (t, 2H), 2.28 (t, 1.4H), 1.97–1.89 (m, 1.4H), and 1.72 (t, 2H).

2.3. Synthesis of PEG and FA modified DCA

The second generation dendrimer (G2), which had 80 peripheral methacrylate groups, was synthesized and characterized by ^{1}H NMR and GPC as we previously reported [31]. DTPA–NHS was synthesized and stored in DMSO solution at a DTPA–NHS concentration of 0.72 mmol/mL.

2.3.1. FA-PEG-G2-DTPA

G2 (0.4 g, 0.0137 mmol, 1.09 mmol methacrylate group) and FA-PEG-SH (0.525 g, 0.205 mmol) were dissolved in 6 mL DMSO. For the terminal thiol of PEG had very low activity with macromolecules, not all the PEG chain could react with the dendrimer, thus an excess of PEG was added into the reaction. A catalyst tributyl phosphine (100 μL 0.4 mmol) was then added into the mixture. The solution was stirred at room temperature in dark for 1 day, and then cysteamine (0.0844 g, 1.09 mmol) and DTPA–NHS solution (6 mL, containing 4.32 mmol DTPA–NHS) were successively added into the mixture within an interval of 1 h, and stirred for another 12 h. The mixture was purified by dialysis in methanol for 2 days in dark. The solvent was removed by rotary evaporation. The product FA-PEG-G2-DTPA was obtained after drying under vacuum with a yield of 45% (0.604 g). ^{1}H NMR in D_2O (pH = 7), δ_{ppm}: 8.66 (s, 7H), 7.57 (d, 14H), 6.70 (d, 14H), 4.32 (s, 480H), 3.73 (s, 552H), 3.59 (s, 1975H), 3.30 (t, 276H), 3.21 (s, 138H), 3.12 (t, 276H), 2.97 (t, 260H), 2.86–2.60 (m, 1040H), and 1.15 (s, 420H).

2.3.2. FA-PEG-G2-DTPA-Gd

FA-PEG-G2-DTPA (0.2 g) was added into a solution of gadolinium chloride hexahydrate (1.89 mmol Gd, 1.2 eq.) in 0.1 M sodium acetate buffer solution (pH = 7). After the solution was stirred at room temperature for 1 h, it was filtered by Amicon® Ultra-15 (MWCO

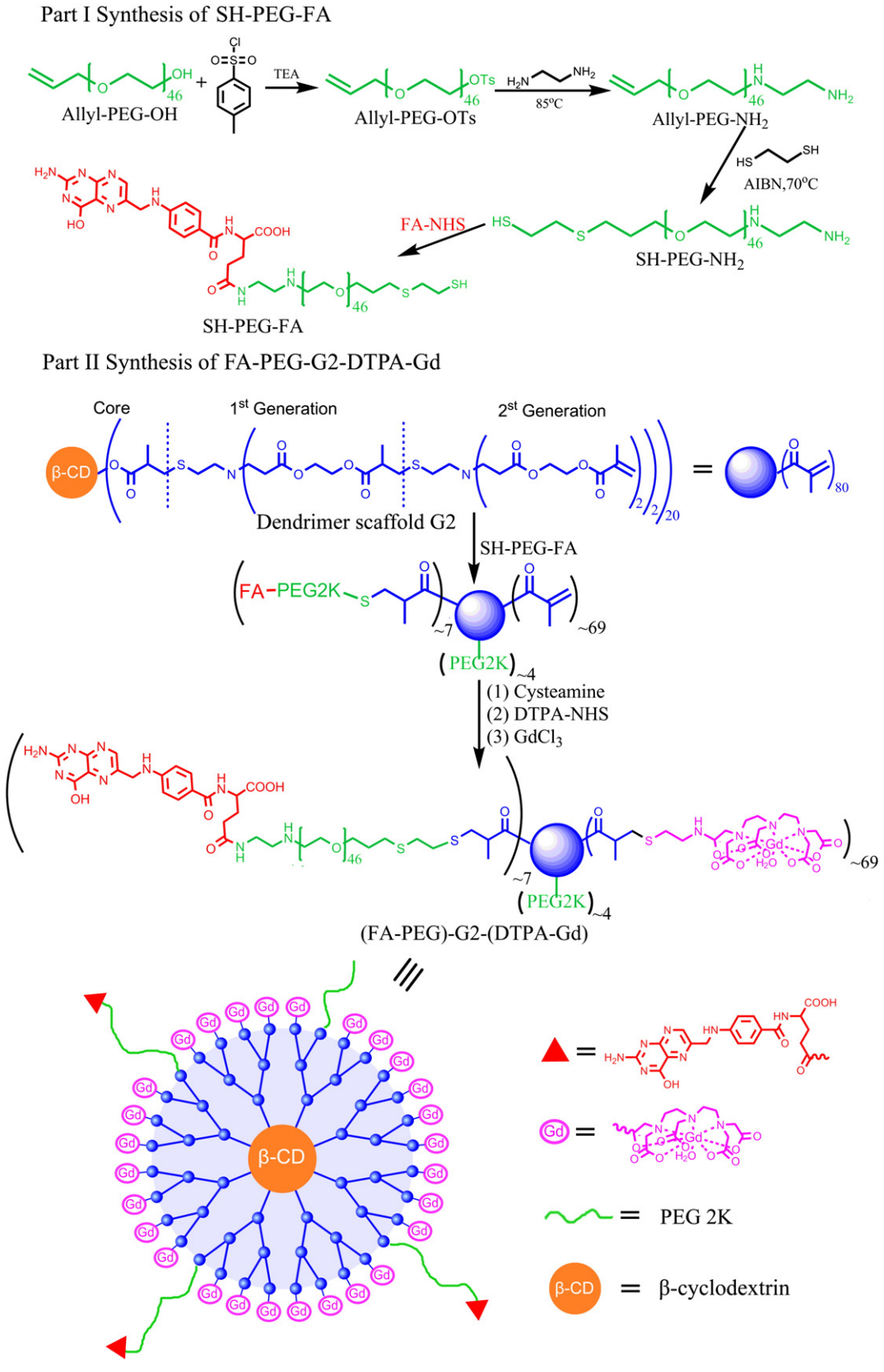

Fig. 1. Schematic illustration of the synthesis of the tumor targeting dendritic MRI contrast agent.

10,000) four times to remove the excess Gd^{3+}. The remained solution was then lyophilized, yielding FA-PEG-G2-DTPA-Gd as a yellowish floccule of 0.121 g (54%).

2.3.3. PEG-G2-DTPA-Gd

The synthesis of PEG-G2-DTPA and PEG-G2-DTPA-Gd followed the same method using OH-PEG-SH instead of FA-PEG-SH. ^{1}H NMR

of PEG-G2-DTPA in D_2O, δ_{ppm}: 4.32 (s, 480H), 3.77 (s, 544H), 3.59 (s, 2147H), 3.46 (s, 136H), 3.36 (t, 272H), 3.27 (s, 136H), 3.08 (t, 272H), 2.92 (m, 260H), 2.86–2.60 (m, 1040H), and 1.15 (s, 420H).

2.4. In vitro degradation

FA-PEG-G2-DTPA (14 mg/mL) was incubated in water at different pH with or without esterase (EC 3.1.1.1, 15 U/mL) at 37 °C. Samples were taken at timed intervals, lyophilized and measured by ^{1}H NMR. The degradation of FA-PEG-G2-DTPA was calculated from the integrations of the ester peak of $-CH_2-O-CO-$ at 4.32 ppm and the peak from DTPA at 3.73 ppm in the ^{1}H NMR spectra.

2.5. Measurement of the Gd content in DCAs by titration

The Gd concentrations of samples for R_1 tests were measured using a titration method with arsenazo III as indicator [35]. A weighted DCA sample was digested by 0.5 mL nitric acid for 1 h. Nitric acid was removed by evaporation at 100 °C and the sample was redissolved in acetate buffer (pH = 3.5). 0.1 mL arsenazo III solution (1.2 μM) was added into the sample as indicator and then titrated with DTPA solution (250 mg/L) until the solution color switched from light indigo to tyrian purple.

2.6. Longitudinal relaxivity (R_1) measurement and in vitro MRI

The longitudinal relaxation times (T_1) and in vitro MRI were measured with a 0.52-T MicroMR Imaging & Analyzing System (Shanghai Niumag Corporation, China) at 32 °C. T_1 values of CA solutions with different Gd concentrations ranging from 0.5 to 2 mM in water were measured. The R_1 values of CAs were defined by the formula (1).

$$(1/T_1)_{obs} = (1/T_1)_d + R_1 \cdot [Gd] \quad (1)$$

where [Gd] is the Gd concentration, $(1/T_1)_{obs}$ is the observed relaxation rate, and $(1/T_1)_d$ is the relaxation rate of water protons. The plot of $(1/T_1)_{obs}$ vs [Gd] gave the R_1 as its slope.

For in vitro MRI, the solutions of FA-PEG-G2-DTPA-Gd, PEG-G2-DTPA-Gd and Magnevist were prepared at a Gd concentration of 0.2 mM in 2-cm-diameter test tubes. The samples were measured using a multi-slice spin echo (MSE) sequence. The parameters were set as follows: TR = 300 ms, the effective TE = 1.5 ms and the matrix dimensions = 512 × 512. Signals were recorded by a resonant coil with an inner diameter of 2 cm.

2.7. Tumor model

All animal studies were performed according to the guidelines established by the Institute for Experimental Animals of Zhejiang University. Adult female nude mice at 6-weeks old (average 20 g) were obtained from the Animal Center of Zhejiang University. About 2×10^6 KB cells (human nasopharyngeal epidermoid carcinoma cells) were suspended in 200 μL of PBS and subcutaneously injected into the right lower back of the nude mice. The MRI study was performed when the tumor size reached 5 mm in diameter at day 10.

2.8. In vivo MR imaging

The mice were anesthetized by pentobarbital sodium salt at a dose of 80 mg/kg. Contrast-enhanced imaging of mice was performed on a GE Signa HDx 3T MRI system equipped with a mice coil using a T_1-weighted spin echo (SE) sequence. The imaging parameters were set as follows: TE = 11 ms, TR = 360 ms, bandwidth = 20.83 kHz, FOV = 6 cm and slice thickness = 1.5 mm. The CAs were injected via the tail vein into the anesthetized mice and the images were acquired at 3, 15, 30, 60 and 150 min post injection. The contrast to noise ratio (CNR) was calculated using the following equation: $CNR = (S - S_0)/\sigma_n$, where S (post-injection) and S_0 (pre-injection) were the signals within the regions of interest (about 1.92 mm^2) and σ_n was the standard deviation of noise estimated from the background air. The signal change was evaluated semiquantitatively by plotting the CNR within the tumor versus time. The *P* values were calculated using the Student's two-tailed *t*-test, assuming statistical significance at $P<0.05$.

2.9. Measurement of Gd retention in tissues

A group of 3 ICR mice (6 weeks old) were used to study the subacute Gd retention of FA-PEG-G2-DTPA-Gd in the major organs and tissues. The mice were injected at a dose of 0.1 mmol Gd/kg via the tail vein, and then sacrificed by cervical dislocation at 10 days post injection. The organ and tissue samples, including femur, heart, lungs, liver, muscles, spleen and kidneys, were collected and weighed. The tissue samples were dissolved in ultra-pure nitric acid and liquefied at 100 °C. The solution was fixed to a volume of 5 mL (100 mL for liver) by adding water, and then transferred to a centrifuge tube and centrifuged at 13,000 rpm for 10 min. The Gd concentration in the supernatant was measured by ICP-MS and the average Gd content in each organ or tissue was calculated accordingly. The Gd content in the muscle was calculated with an estimate that the muscle was 40% of body weight [36].

3. Results and discussion

3.1. Synthesis and characterization of the targeted DCAs

In our previous work, the polyester dendrimer has been demonstrated as a good scaffold for Gd chelates [31]. Their large molecular weights and rigid structures provided the DCAs a high R_1 and a long blood circulation time. To obtain a tumor targeting biodegradable DCA, the G2 dendrimer (shown in Fig. 1) with a molecular weight of 29,260 and 80 methacrylate terminals was chosen as the dendrimer scaffold. Polyethylene glycol (PEG) (Mn of 2 kDa) was grafted onto the DCA to further increase its blood circulation time. Folic acid, which targets the overexpressed folate receptors in most tumors, was also introduced onto the DCA as a targeting group. FA-PEG-SH was first synthesized from the bifunctional allyl-PEG-OH in four steps. The final and intermediate products were characterized by ^{1}H NMR spectra (shown in supporting information).

FA-PEG-SH was then grafted onto the G2 dendrimer via the Michael addition reaction between the thiol group in FA-PEG-SH and the methacrylate groups of the dendrimer (Fig. 1). ^{1}H NMR spectrum indicated about 11 of the 80 methacrylate terminal groups were conjugated with PEG chains (about 7 in 11 PEG chains were linked with folic acid) and the rests were turned into amino groups by reacting with cysteamine, and then reacted with an excess DTPA–NHS, producing FA-PEG-G2-DTPA. PEG-G2-DTPA without folic acid for comparison was synthesized similarly using HO-PEG-SH instead of FA-PEG-SH. Both two dendritic ligands were examined by ^{1}H NMR spectra shown in Figs. 4. The appearance of peaks at 4.3 ppm (ester bond), 3.8 ppm (DTPA characteristic peak) and 3.6 ppm (PEG) suggested that both PEG and DTPA were successfully connected to the polyester dendrimer. From the integration of the peaks at 8.7 ppm (folic acid), 4.3 ppm (dendrimer), 3.8 ppm (DTPA) and 3.6 ppm (PEG), the composition of the dendritic ligand was estimated to be $(FA\text{-}PEG)_{11}$-G2-$(DTPA)_{69}$ and $(PEG)_{12}$-G2-$(DTPA)_{68}$, respectively, where the subscript numbers represent the number of functional groups grafted onto the dendrimer, close to those initially designed. The DCAs were finally obtained after the complexation with Gd. The pH of the DCAs in water should be kept at acidic condition to avoid the hydrolysis of CAs during reaction and purification, and the excess $GdCl_3$ was carefully removed. The resultant DCAs were well water-soluble. Fig. 2 shows that the volume-averaged

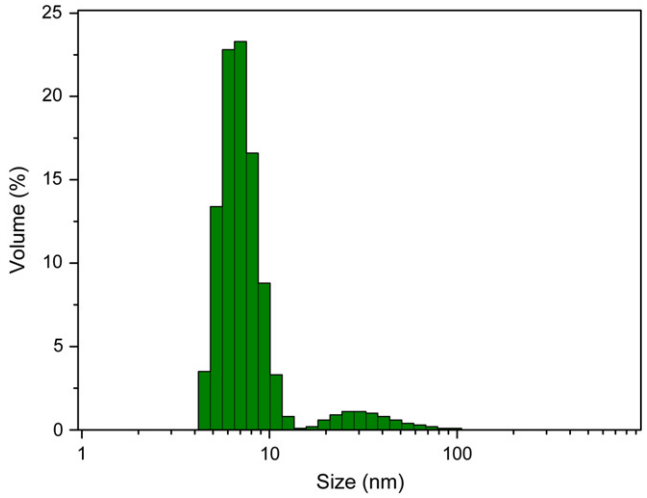

Fig. 2. Size distribution of FA-PEG-G2-DTPA-Gd measured by DLS in water at a DCA concentration of 1 mg/mL.

hydrodynamic diameter of FA-PEG-G2-DTPA-Gd was 7.6 nm with a little aggregate of an average size of 30 nm, and PEG-G2-DTPA-Gd had a similar size and distribution.

3.2. In vitro degradation of the dendritic ligand

The biodegradability was tested by monitoring the hydrolysis of the ester bonds in the dendritic ligand. The integration ratio between the ester bond and DTPA in ^{1}H NMR was used to calculate the hydrolysis kinetics (Fig. 3). The hydrolysis was pH dependent. FA-PEG-G2-DTPA was relatively stable at pH 5.0 with more than 93% ester bonds remained after 10 h hydrolysis, while it hydrolyzed very quickly at the physiological pH (pH = 7.4) with only 70% ester bonds left at the same time point. Moreover, the hydrolysis could be accelerated by adding esterase 15 U/mL, which is abundant in cytoplasm, with only 53% ester bond remained after 10 h. The results illustrate that the polyester dendrimer based DCA can be degraded in the simulated physiological environment.

3.3. R_1s and in vitro MRI

The T_1s of DCA solutions were determined on a 0.52-T MR system at 32 °C and the R_1s were calculated from the slope of the curves of $1/T_1$ against the Gd concentration shown in Fig. 4a. The R_1s of FA-PEG-G2-DTPA-Gd and PEG-G2-DTPA-Gd were 17.1 mM^{-1} s^{-1} and

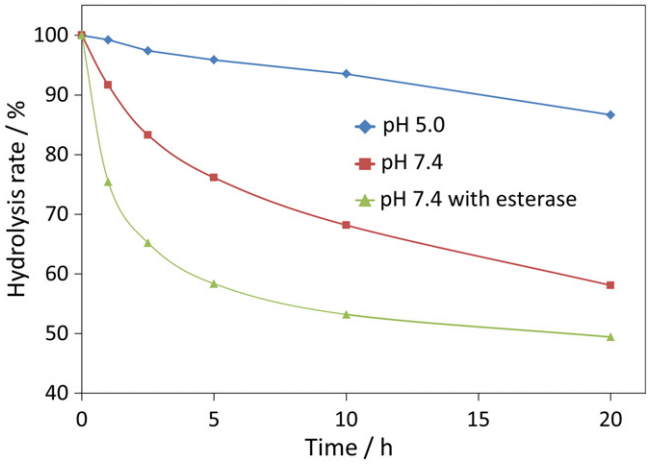

Fig. 3. Hydrolysis kinetics of FA-PEG-G2-DTPA at different pH values with and without esterase at 37 °C and a concentration of 14 mg/mL (esterase concentration, 15 U/mL).

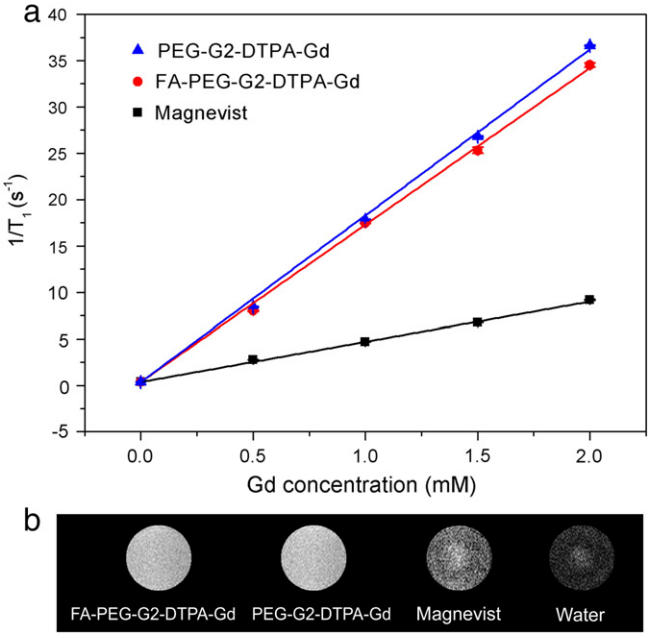

Fig. 4. In vitro R_1s (a) and T_1-weighted MRI (b) of the MRI CAs in water at 0.52 T and 32 °C. The Gd concentration for in vitro MRI was 0.2 mM.

18.2 mM^{-1} s^{-1} per Gd, or 1180 mM^{-1} s^{-1} and 1238 mM^{-1} s^{-1} per molecule, respectively. The ionic R_1s were about 4 times higher than that of the commercially used CA Magnevist (Gd-DTPA). This suggests that the DCA could have much higher imaging enhancement than Magnevist. The high R_1s of the DCAs might be mainly due to that the conjugation of Gd chelate onto the dendrimers increased the rotational correlation time (τ_R) owing to the rigidity of dendrimers [37]. Interestingly, these R_1s were even significantly higher than those of the DCAs with the same dendrimer structure but without PEGylation (G2-DTPA-Gd, 11.7 mM^{-1} s^{-1}) [31]. It was generally expected that PEGylation would decrease R_1s of DCAs because PEG chains might hinder the water exchange between the coordinated H_2O and bulk H_2O, prolonging the residence lifetime of the coordinated H_2O (τ_m) [38,39]. For instance, after PEGylation the R_1 of the DCA based on 4th generation PAMAM decreased from 31 mM^{-1} s^{-1} to 23 mM^{-1} s^{-1} [40]. The R_1 increase by PEGylation in this study was probably due to the increased solubility and rigidity of the DCAs [38]. Fig. 4b shows the T_1-weighted MR images of the CA solutions at the same Gd concentration of 0.2 mM. Obviously, both two DCAs showed much brighter images than the clinically used Magnevist, indicating that the DCAs had much higher contrast efficiency over Magnevist.

3.4. Contrast enhanced in vivo tumor imaging

To examine the efficiency of the targeted DCAs to enhance in vivo MRI of tumor, nude mice inoculated with human KB tumors were intravenously injected with FA-PEG-G2-DTPA-Gd, PEG-G2-DTPA-Gd or Magnevist, respectively, at the same dose of 0.1 mmol Gd/kg, and their MRI was acquired on a 3-T MRI system. Axial MR images acquired pre-injection and at various time points after the injection are shown in Fig. 5a. All the tumors contrasted by FA-PEG-G2-DTPA-Gd, PEG-G2-DTPA-Gd and Magnevist were significantly brighter than the surrounding tissues, which made the tumor delineated clearly. Moreover, the tumors contrasted by the DCAs were much brighter than those contrasted by Magnevist (Fig. 5a). To quantitatively analyze of the signal change, the contrast-to-noise ratio (CNR) in tumor at different points was measured (Fig. 5b). The tumors contrasted by the DCAs had much higher CNR than those with Magnevist at all time points. For instance, the maximum CNRs in tumors with the DCAs were about twice higher than those with Magnevist. The higher CNR in tumor contrasted by

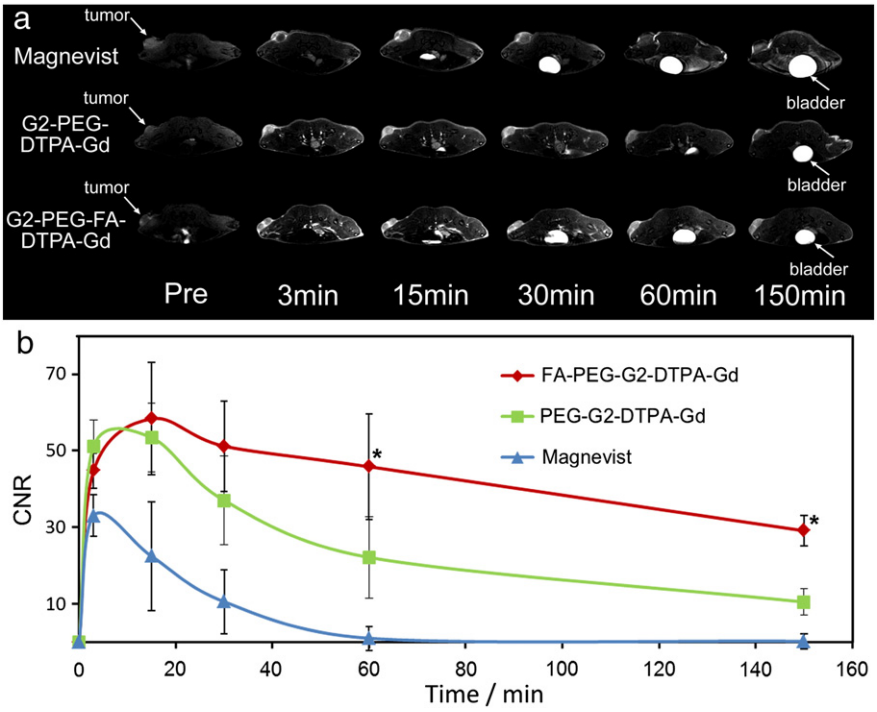

Fig. 5. 2D axial images (a) and contrast-to-noise ratio (CNR) (b) of tumors in mice injected with FA-PEG-G2-DTPA-Gd, PEG-G2-DTPA-Gd or Magnevist at 0.1 mmol/kg. The values are expressed as the mean and the standard deviation (n = 3). The asterisk indicates significant differences between DCA and Magnevist ($P<0.05$).

DCAs was due to their higher R_1s and accumulation in tumor via the EPR effect. Moreover, while the brightness of the tumor with Magnevist started to decline at 5 min post injection, that with the DCAs started to decrease at 15 min post injection, which was also clearly indicated by the CNR decrease in Fig. 5b. The CNR declination in tumors with the DCAs was due to their biodegradation and resultant excretion via kidney, which can be traced by the increasing brightness in the bladder. Interestingly, while the CNRs of tumors with PEG-G2-DTPA-Gd and Magnevist decreased quickly, the CNRs of tumor with FA-PEG-G2-DTPA-Gd decayed slowly. At 60 min post injection, the contrast between tumor and surrounding tissues in mice with PEG-G2-DTPA-Gd and Magnevist was already weak but the contrast in mice with FA-PEG-G2-DTPA-Gd was still strong, while the signal in normal tissues deceased with the excretion of CAs. Thus, the tumor could be markedly identified from normal tissues and its boundary could be clearly demarcated. The significantly long retention of FA-PEG-G2-DTPA-Gd in tumor was due to the ligand-mediated uptake of dendritic CAs into the cancer cells. In contrast, PEG-G2-DTPA-Gd hardly entered cells, and thus had much shorter retention in tumor.

3.5. Gd retention in tissues

The accumulated CAs in body might be internalized by healthy cells and metabolized into toxic Gd^{3+} ions, which may cause hepatocellular necrosis, lymphoid depletion, nephrogenic systemic fibrosis (NSF) and mineralization in the spleen [24–26]. Therefore, the Gd accumulation is considered as an important parameter to evaluate a MRI CA. The Gd retention in major organs and tissues including heart, femur, spleen, muscles, lungs, kidneys and liver is shown in Fig. 6. FA-PEG-G2-DTPA-Gd had much lower Gd retention than the non-degradable DCA PAMAM-G6-(Gd-DO3A) [23] in all the organs or tissues. The accumulation in femur, muscles and especially kidneys was even lower than that of in the clinically used small molecule CA Gd-(DTPA-BMA) [29] except that the Gd residue in liver was slightly higher than that of Gd-(DTPA-BMA). Such low Gd retentions were consistent with the results of the polydisulfide based biodegradable macromolecular CA [29], verified that the DCAs based on polyester dendrimers could be hydrolyzed in vivo and excreted out of the body, excluding the risk from the subacute accumulation of macromolecular CAs.

4. Conclusions

A tumor-targeting DCA (FA-PEG-G2-DTPA-Gd) was prepared from a polyester dendrimer through grafting PEG with a distal folic acid and conjugation of Gd chelates. FA-PEG-G2-DTPA-Gd had an average hydrodynamic diameter of 7.6 nm. It was relatively stable in acidic solution, but degradable under the physiological pH and the hydrolysis could be further accelerated in presence of esterase. The DCA had a high R_1 up to 17.1 mM^{-1} s^{-1}, 1.6 times higher than the unPEGylated one and 4 times higher than Magnevist. In vivo evaluation showed that the DCA had much higher contrast enhancement in tumor than Magnevist,

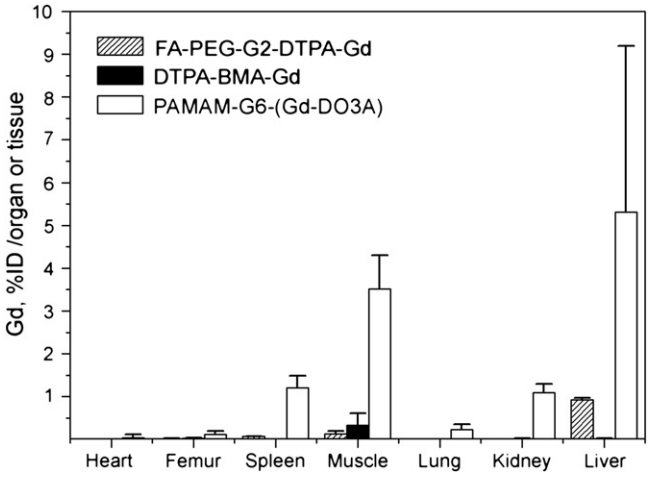

Fig. 6. Retention of Gd in mice 10 days after i.v. injection of FA-PEG-G2-DTPA-Gd, Gd-(DTPA-BMA)* and PAMAM-G6-(Gd-DO3A)* at a dose of 0.1 mmol Gd/kg. *The data of Gd-(DTPA-BMA) and PAMAM-G6-(Gd-DO3A) were from literature [23,29].

and its enhancement lasted a much longer time. The subacute Gd retention measurement showed that FA-PEG-G2-DTPA-Gd had much lower Gd retention than the non-degradable DCAs in all the organs or tissues. The high efficiency in MRI contrast enhancement and low Gd retention made it promising CA for contrast-enhanced tumor MRI.

Acknowledgments

This work was financially supported by the National Nature Science Foundation of China (20904046, 21174128, 50888001, 21090352), the Doctoral Fund of Ministry of Education of China (20090101120159), the Qianjiang Talent Program of Zhejiang Province, China (2010R10050), and the Program for Changjiang Scholars and Innovative Research Team in University (IRT0942).

Appendix A. Supplementary data

Supplementary data to this article can be found online at http://dx.doi.org/10.1016/j.jconrel.2013.01.034.

References

[1] A. Jemal, F. Bray, M.M. Center, J. Ferlay, E. Ward, D. Forman, Global cancer statistics, CA Cancer J. Clin. 61 (2011) 69–90.
[2] C.M. Balch, A.C. Buzaid, S.J. Soong, M.B. Atkins, N. Cascinelli, D.G. Coit, I.D. Fleming, J.E. Gershenwald, A. Houghton, J.M. Kirkwood, K.M. McMasters, M.F. Mihm, D.L. Morton, D.S. Reintgen, M.I. Ross, A. Sober, J.A. Thompson, J.F. Thompson, Final version of the American Joint Committee on Cancer staging system for cutaneous melanoma, J. Clin. Oncol. 19 (2001) 3635–3648.
[3] J. Bruix, J.M. Llovet, Prognostic prediction and treatment strategy in hepatocellular carcinoma, Hepatology 35 (2002) 519–524.
[4] S.J. Nelson, Analysis of volume MRI and MR spectroscopic imaging data for the evaluation of patients with brain tumors, Magn. Reson. Med. 46 (2001) 228–239.
[5] K. Nakanishi, M. Kobayashi, K. Nakaguchi, M. Kyakuno, N. Hashimoto, H. Onishi, N. Maeda, S. Nakata, M. Kuwabara, T. Murakami, H. Nakamura, Whole-body MRI for detecting metastatic bone tumor: diagnostic value of diffusion-weighted images, Magn. Reson. Med. Sci. 6 (2007) 147–155.
[6] P. Caravan, J.J. Ellison, T.J. McMurry, R.B. Lauffer, Gadolinium(III) chelates as MRI contrast agents: structure, dynamics, and applications, Chem. Rev. 99 (1999) 2293–2352.
[7] M.F. Bellin, MR contrast agents, the old and the new, Eur. J. Radiol. 60 (2006) 314–323.
[8] H.J. Weinmann, R.C. Brasch, W.R. Press, G.E. Wesbey, Characteristics of gadolinium-DTPA complex — a potential NMR contrast agent, Am. J. Roentgenol. 142 (1984) 619–624.
[9] V. Comblin, D. Gilsoul, M. Hermann, V. Humblet, V. Jacques, M. Mesbahi, C. Sauvage, J.F. Desreux, Designing new MRI contrast agents: a coordination chemistry challenge, Coord. Chem. Rev. 185–6 (1999) 451–470.
[10] M.W. Brechbiel, A.J.L. Villaraza, A. Bumb, Macromolecules, dendrimers, and nanomaterials in magnetic resonance imaging: the interplay between size, function, and pharmacokinetics, Chem. Rev. 110 (2010) 2921–2959.
[11] H. Maeda, J. Wu, T. Sawa, Y. Matsumura, K. Hori, Tumor vascular permeability and the EPR effect in macromolecular therapeutics: a review, J. Control. Release 65 (2000) 271–284.
[12] A.L. Doiron, K. Chu, A. Ali, L. Brannon-Peppas, Preparation and initial characterization of biodegradable particles containing gadolinium-DTPA contrast agent for enhanced MRI, Proc. Natl. Acad. Sci. U. S. A. 105 (2008) 17232–17237.
[13] Z.R. Lu, D.L. Parker, K.C. Goodrich, X.H. Wang, J.G. Dalle, H.R. Buswell, Extracellular biodegradable macromolecular gadolinium(III) complexes for MRI, Magn. Reson. Med. 51 (2004) 27–34.
[14] H. Daldrup, D.M. Shames, M. Wendland, Y. Okuhata, T.M. Link, W. Rosenau, Y. Lu, R.C. Brasch, Correlation of dynamic contrast-enhanced MR imaging with histologic tumor grade: comparison of macromolecular and small-molecular contrast media, Am. J. Roentgenol. 171 (1998) 941–949.
[15] A. Gossmann, Y. Okuhata, D.M. Shames, T.H. Helbich, T.P.L. Roberts, M.F. Wendland, S. Huber, R.C. Brasch, Prostate cancer tumor grade differentiation with dynamic contrast-enhanced MR imaging in the rat: comparison of macromolecular and small-molecular contrast media — preliminary experience, Radiology 213 (1999) 265–272.
[16] Y. Feng, E.K. Jeong, A.M. Mohs, L. Emerson, Z.-R. Lu, Characterization of tumor angiogenesis with dynamic contrast-enhanced MRI and biodegradable macromolecular contrast agents in mice, Magn. Reson. Med. 60 (2008) 1347–1352.
[17] A. Gossmann, T.H. Helbich, N. Kuriyama, S. Ostrowitzki, T.P.L. Roberts, D.M. Shames, N. van Bruggen, M.F. Wendland, M.A. Israel, R.C. Brasch, Dynamic contrast-enhanced magnetic resonance imaging as a surrogate marker of tumor response to anti-angiogenic therapy in a xenograft model of glioblastoma multiforme, J. Magn. Reson. Imaging 15 (2002) 233–240.
[18] C.D. Pham, T.P.L. Roberts, N. van Bruggen, O. Melnyk, J. Mann, N. Ferrara, R.L. Cohen, R.C. Brasch, Magnetic resonance imaging detects suppression of tumor vascular permeability after administration of antibody to vascular endothelial growth factor, Cancer Invest. 16 (1998) 225–230.
[19] A. Tsourkas, Z.L. Cheng, D.L.J. Thorek, Gadolinium-conjugated dendrimer nanoclusters as a tumor-targeted T(1) magnetic resonance imaging contrast agent, Angew. Chem. Int. Edit. 49 (2010) 346–350.
[20] S.D. Konda, M. Aref, S. Wang, M. Brechbiel, E.C. Wiener, Specific targeting of folate-dendrimer MRI contrast agents to the high affinity folate receptor expressed in ovarian tumor xenografts, Magn. Reson. Math. Phys. Biol. Med. 12 (2001) 104–113.
[21] E.C. Wiener, S. Konda, A. Shadron, M. Brechbiel, O. Gansow, Targeting dendrimer-chelates to tumors and tumor cells expressing the high-affinity folate receptor, Invest. Radiol. 32 (1997) 748–754.
[22] H. Kobayashi, N. Sato, S. Kawamoto, T. Saga, A. Hiraga, T.L. Haque, T. Ishimori, J. Konishi, K. Togashi, M.W. Brechbiel, Comparison of the macromolecular MR contrast agents with ethylenediamine-core versus ammonia-core generation-6 polyamidoamine dendrimer, Bioconjug. Chem. 12 (2001) 100–107.
[23] R.Z. Xu, Y.L. Wang, X.L. Wang, E.K. Jeong, D.L. Parker, Z.R. Lu, In vivo evaluation of a PAMAM-Cystamine-(Gd-DO3A) conjugate as a biodegradable macromolecular MRI contrast agent, Exp. Biol. Med. 232 (2007) 1081–1089.
[24] W.P. Cacheris, S.C. Quay, S.M. Rocklage, The relationship between thermodynamics and the toxicity of gadolium complexes, Magn. Reson. Imaging 8 (1990) 467–481.
[25] A. Spencer, S. Wilson, E. Harpur, Gadolinium chloride toxicity in the mouse, Hum. Exp. Toxicol. 17 (1998) 633–637.
[26] K. Nwe, M. Bernardo, C.A.S. Regino, M. Williams, M.W. Brechbiel, Comparison of MRI properties between derivatized DTPA and DOTA gadolinium-dendrimer conjugates, Bioorg. Med. Chem. 18 (2010) 5925–5931.
[27] Y. Zong, X. Wang, E.-K. Jeong, D.L. Parker, Z.-R. Lu, Structural effect on degradability and in vivo contrast enhancement of polydisulfide Gd(III) complexes as biodegradable macromolecular MRI contrast agents, Magn. Reson. Imaging 27 (2009) 503–511.
[28] A.M. Mohs, X.H. Wang, K.C. Goodrich, Y.D. Zong, D.L. Parker, Z.R. Lu, PEG-g-poly(GdDTPA-co-L-cystine): a biodegradable macromolecular blood pool contrast agent for MR imaging, Bioconjug. Chem. 15 (2004) 1424–1430.
[29] X.H. Wang, Y. Feng, T.Y. Ke, M. Schabel, Z.R. Lu, Pharmacokinetics and tissue retention of (Gd-DTPA)-cystamine copolymers, a biodegradable macromolecular magnetic resonance imaging contrast agent, Pharm. Res. 22 (2005) 596–602.
[30] Y.Q. Shen, X.P. Ma, J.B. Tang, M.H. Fan, H.D. Tang, M. Radosz, Facile synthesis of polyester dendrimers from sequential click coupling of asymmetrical monomers, J. Am. Chem. Soc. 131 (2009) 14795–14803.
[31] M. Ye, Y. Qian, Y. Shen, H. Hu, M. Sui, J. Tang, Facile synthesis and in vivo evaluation of biodegradable dendritic MRI contrast agents, J. Mater. Chem. 22 (2012) 14369–14377.
[32] J. Heyes, K. Hall, V. Tailor, R. Lenz, I. MacLachlan, Synthesis and characterization of novel poly(ethylene glycol)-lipid conjugates suitable for use in drug delivery, J. Control. Release 112 (2006) 280–290.
[33] T. Hirasawa, Y. Maeda, H. Kitano, Inclusional complexation by cyclodextrin-polymer conjugates in organic solvents, Macromolecules 31 (1998) 4480–4485.
[34] G. Pasut, F. Canal, L.D. Via, S. Arpicco, F.A. Veronese, O. Schiavon, Antitumoral activity of PEG-gemcitabine prodrugs targeted by folic acid, J. Control. Release 127 (2008) 239–248.
[35] H. Rohwer, N. Collier, E. Hosten, Spectrophotometric study of arsenazo-III and its interactions with lanthanides, Anal. Chim. Acta 314 (1995) 219–223.
[36] D.J. Parmelee, R.C. Walovitch, H.S. Ouellet, R.B. Lauffer, Preclinical evaluation of the pharmacokinetics, biodistribution, and elimination of MS-325, a blood pool agent for magnetic resonance imaging, Invest. Radiol. 32 (1997) 741–747.
[37] G.M. Nicolle, E. Toth, H. Schmitt-Willich, B. Raduchel, A.E. Merbach, The impact of rigidity and water exchange on the relaxivity of a dendritic MRI contrast agent, Chem. Eur. J. 8 (2002) 1040–1048.
[38] E. Toth, I. van Uffelen, L. Helm, A.E. Merbach, D. Ladd, K. Briley-Saebo, K.E. Kellar, Gadolinium-based linear polymer with temperature-independent proton relaxivities: a unique interplay between the water exchange and rotational contributions, Magn. Reson. Chem. 36 (1998) S125–S134.
[39] D.M.J. Doble, M. Botta, J. Wang, S. Aime, A. Barge, K.N. Raymond, Optimization of the relaxivity of MRI contrast agents: effect of poly(ethylene glycol) chains on the water-exchange rates of Gd-III complexes, J. Am. Chem. Soc. 123 (2001) 10758–10759.
[40] C. Kojima, B. Turkbey, M. Ogawa, M. Bernardo, C.A.S. Regino, L.H. Bryant Jr., P.L. Choyke, K. Kono, H. Kobayashi, Dendrimer-based MRI contrast agents: the effects of PEGylation on relaxivity and pharmacokinetics, Nanomedicine Nanotechnol. 7 (2011) 1001–1008.